Curcumin-conjugated nanoliposomes with high affinity for Aβ deposits: Possible applications to Alzheimer disease

ARTICLE *in* NANOMEDICINE: NANOTECHNOLOGY, BIOLOGY, AND MEDICINE · DECEMBER 2012

Impact Factor: 6.16 · DOI: 10.1016/j.nano.2012.11.004 · Source: PubMed

POTENTIAL CLINICAL RELEVANCE

Nanomedicine: Nanotechnology, Biology, and Medicine
9 (2013) 712–721

Original Article

nanomedjournal.com

Curcumin-conjugated nanoliposomes with high affinity for Aβ deposits: Possible applications to Alzheimer disease

Adina N. Lazar, PhD[a,b], Spyridon Mourtas, PhD[c], Ihsen Youssef, PhD[b], Christophe Parizot, MS[d], Aurélien Dauphin, PhD[e], Benoît Delatour, PhD[b], Sophia G. Antimisiaris, PhD[c,f], Charles Duyckaerts, MD, PhD[a,b,*]

[a]*Laboratoire de Neuropathologie Escourolle, Hôpital de la Salpêtrière, AP-HP, 47 Bd de l'Hôpital, Paris, France*
[b]*Centre de recherche de l'ICM, (UPMC, INSERM UMR S 975, CNRS UMR 7225), 47 Bd de l'Hôpital, Paris, France*
[c]*Laboratory of Pharmaceutical Technology, Dept. of Pharmacy, School of Health Sciences, University of Patras, Rio, Greece*
[d]*Département d'Immunologie Cellulaire et Tissulaire, CERVI INSERM U 945, Hôpital Pitié-Salpêtrière, 83 Boulevard de l'Hôpital, Paris, France*
[e]*Plateforme d'Imagerie cellulaire Pitié-Salpêtrière, 47 Bd de l'Hôpital, Paris, France*
[f]*Institute of Chemical Engineering and Sciences, FORTH/ICES, Rio Patras, Greece*

Received 1 June 2012; accepted 13 November 2012

Abstract

Accumulation of amyloid peptide (Aβ) in senile plaques is a hallmark lesion of Alzheimer disease (AD). The design of molecules able to target the amyloid pathology in tissue is receiving increasing attention, both for diagnostic and for therapeutic purposes. Curcumin is a fluorescent molecule with high affinity for the Aβ peptide but its low solubility limits its clinical use. Curcumin-conjugated nanoliposomes, with curcumin exposed at the surface, were designed. They appeared to be monodisperse and stable. They were non-toxic in vitro, down-regulated the secretion of amyloid peptide and partially prevented Aβ-induced toxicity. They strongly labeled Aβ deposits in post-mortem brain tissue of AD patients and APPxPS1 mice. Injection in the hippocampus and in the neocortex of these mice showed that curcumin-conjugated nanoliposomes were able to specifically stain the Aβ deposits in vivo. Curcumin-conjugated nanoliposomes could find application in the diagnosis and targeted drug delivery in AD.

From the Clinical Editor: In this preclinical study, curcumin-conjugated nanoliposomes were investigated as possible diagnostics and targeted drug delivery system in Alzheimer's disease, demonstrating strong labeling of Aβ deposits both in human tissue and in mice, and in vitro downregulation of amyloid peptide secretion and prevention of Aβ-induced toxicity.

Key words: Curcumin; Curcumin-conjugated nanoliposomes; Alzheimer disease; Amyloid peptide; Amyloid deposits

This work was supported by the European Community's Seventh Framework Programme (FP7/2007-2013) under grant agreement no. 212043. The funding source had no involvement in the study design, data collection and analysis or the writing of the report and the decision to submit the paper for publication. We thank GIE NeuroCEB Brain Bank for providing the human brain samples. A grant from "Projet Hospitalier de Recherche Clinique" (PHRC) IMAD helped us in analyzing post-mortem tissue. This work has received financial support from the program "Investissements d'Avenir" ANR-10-IAIHU-06. The expertise of the technical staff of Escourolle Neuropathology Laboratory is greatly acknowledged. Confocal images have been taken using the Plateforme d'Imagerie Cellulaire du CR-ICM, Hôpital de la Pitié-Salpêtrière.

No conflicts of interest to be declared.

*Corresponding author: Laboratoire de Neuropathologie Escourolle and Centre de Recherche de l'ICM, (UPMC, INSERM UMR S 975, CNRS UMR 7225), Hôpital de la Salpêtrière, AP-HP, 47 Bd de l'Hôpital, 75013 Paris, France.

E-mail address: charles.duyckaerts@psl.aphp.fr (C. Duyckaerts).

1549-9634/$ – see front matter © 2013 Elsevier Inc. All rights reserved.
http://dx.doi.org/10.1016/j.nano.2012.11.004

Extracellular deposits of Aβ peptide (e.g. in senile plaques) and intraneuronal accumulations of tau protein (e.g. in neurofibrillary tangles) are the main histopathological features of AD.[1] Aβ deposits are present in the cortical gray matter, years before the onset of dementia. Radiolabeled molecules with high affinity for Aβ, such as Pittsburgh compound B (PIB)[2] or ^{18}F-AV-45,[3] are currently used for in vivo detection. New means of reaching senile plaques in vivo, such as nanoparticles that could embark diagnostic and therapeutic agents are developed. We chose liposomes as a particularly versatile vehicle and curcumin as an Aβ-targeting molecule. Curcumin and curcumin derivatives are indeed known to bind Aβ deposits in vivo, in vitro or in post-mortem tissue.[4–7]

Nanoparticle-based delivery has the potential of rendering hydrophobic agents, such as curcumin, dispersible in aqueous media. Liposomes are non-toxic and non-immunogenic, fully biodegradable and structurally versatile nanoparticles.[8–12] They

Please cite this article as: Lazar AN, et al, Curcumin-conjugated nanoliposomes with high affinity for Aβ deposits: Possible applications to Alzheimer disease. *Nanomedicine: NBM* 2013;9:712-721, http://dx.doi.org/10.1016/j.nano.2012.11.004

Table 1
Nanoliposomes formulations and their physicochemical properties.

Liposome type	Liposome name	DPS–curcumin in liposomes (mol%)	PI[a]	ζ-Potential (mV)	Mean diameter (nm)
DPPC/Chol (2:1)+DPS–curcumin	Curcumin-conjugated nanoliposomes (CnLs)	20[b]	0.255	−10.5±1.2	207.2±8.0
DPPC/Chol (2:1)+FITC–dextran (encapsulated)	FITC nanoliposomes	0	0.232	−9.8±3.2	198.5±9.8
DPPC/Chol (2:1)	Nude nanoliposomes	0	0.195	−6.44±0.49	63.1±6.2

[a] PI=polydispersity index.
[b] Total ratio (mol/mol/mol): DPPC/Chol/DPS–curcumin (59:29:12).

may be loaded with contrast probes or therapeutic agents. Their surface is easily customed to direct them to specific targets[13] or to help their crossing the blood–brain barrier (BBB).[14–16]

We report the design of biocompatible curcumin-conjugated nanoliposomes (CnLs) with high affinity for amyloid deposits. This is the first step in the development of new nanoparticles, with application in AD diagnosis or treatment.

Materials and methods

Curcumin–phospholipid conjugate synthesis

The synthesis of curcumin–phospholipid conjugate, 1,2-dipalmitoyl-3-(2-(1,7-*bis*(4-hydroxy-3-methoxyphenyl)-3,5-dioxohept-6-enylthio)ethyl phospho)-*sn*-glycerol (DPS–curcumin) was performed via Michael addition of curcumin,[17] using 1,2-dipalmitoyl-*sn*-glycero-3-phosphothioethanol (sodium salt) (DPSH) as nucleophile in the presence of *N*,*N*-diisopropylethylamine (DIPEA). Briefly, DPSH (1 eq) was added slowly to a solution of curcumin (3 eq) and DIPEA within 2–3 h. The mixture was further reacted at room temperature for 24 h (under N_2 flow in order to avoid any DPSH disulfide formation). The conversion of DPSH to DPS–curcumin was monitored by thin layer chromatography (TLC). The reaction mixture was subjected to purification using a silica gel column and mixtures of $CHCl_3$/MeOH as eluents (40/1, 30/1, 20/1, 15/1, 12.5/1, 10/1, 7.5/1, 5/1, 4/1, 3/1, MeOH). Fractions 5/1 and 4/1 were combined and concentrated under reduced pressure. TLC analysis showed a single UV/vis, molybdene blue spray and I_2 positive spot (yield: 75%) and the product was further analyzed by NMR, HPLC and ESI-MS.

DPS–curcumin characterization by NMR, HPLC and ESI-MS

^{1}H-NMR and ^{13}C-NMR spectra were recorded at 293 K on a Brucker spectrometer 400 MHz using methanol-d4 (CD_3OD) and chloroform-d ($CDCl_3$) as solvents and TMS as internal standard. The HPLC analysis was performed on a Shimadzu UPLC. The lipid was dissolved in the mobile phase (chloroform/methanol [9:1] containing 0.08% TFA—isocratic elution) and the solution was injected on a Lichrosphere 100RP-18 (5 μm) column and eluted at a flow rate of 1 ml/min; the detection wavelength was set to 380 nm. The lipid was collected at the exit of the HPLC column and subjected to ESI-MS analysis. ESI-MS was performed with an electrospray platform (Waters) equipped with a Masslynx NT 2.3 operational system.

Nanoliposomes formulation

CnLs were prepared from 1,2-dipalmitoyl-*sn*-glycerol-3-phosphatidylcholine (DPPC), cholesterol (Chol) and DPS–curcumin. The appropriate amount of lipids, for a final ratio of DPPC/Chol (2:1) with 20 mol% DPS–curcumin (in respect to DPPC), was dissolved in chloroform/methanol (2:1) and mixed. The solvent was evaporated under vacuum until the formation of a thin lipid layer on the walls of the glass container. The lipid film was further treated with N_2, to remove any traces of organic solvent and subsequently hydrated in PBS buffer (pH 7.4) at 45 °C. After complete lipid hydration, the suspension of vesicles was placed under the microtip of a sonicator probe until the nanoliposome dispersion was completely clear. The final phospholipid concentration was 2 mg/ml, as assessed by the thiocyanate method of Stewart,[18] used as a proxy measure of liposomes concentration. FITC nanoliposomes (DPPC/Chol vesicles encapsulating FITC–dextran) as well as nude nanoliposomes (DPPC/Chol, without fluorochrome), serving as controls, were also prepared by the same protocol (Table 1).

Characterization of nanoliposomes

A Malvern Nanosizer (particle sizer and ζ-potential analyzer) was used to characterize the nanoliposomes. Vesicle size distribution was assessed by dynamic light scattering with a 625-nm laser beam, at 25 °C. Size and polydispersity indices were obtained from the intensity autocorrelation function of the light scattered at a fixed angle of 173° (conditions that avoid errors due to back-scattering). The ζ-potential was measured at 25 °C. The stability of the size of CnLs, FITC nanoliposomes and nude nanoliposomes was also determined by flow cytometry. A Gallios® cytometer (Beckman Coulter), particularly suited for the detection of small particles, was used.

Cytotoxicity assay and cytotoxicity prevention by CnLs

To evaluate the cytotoxicity of CnLs, HEK cells (from Human Embryonic Kidney), control SH-SY5Y cells (human neuroblastoma cells) and $hAPP_{sw}$ SH-SY5Y cells stably overexpressing the human APP gene (hAPP) bearing the Swedish mutation (causing familial Alzheimer disease) were used. The cells were seeded in multiwell culture plates and grown in culture medium until approximately 80% confluence. The growth medium was then discarded and the cells were incubated for 24 h in a culture medium enriched in CnLs (final concentration 20 μg/ml). The cytotoxicity was assessed by means of MTT, based on the conversion of tetrazolium salt (MTT) into a purple formazan product.[19] Control

SH-SY5Y cells were used for determining the capacity of CnLs to prevent the toxicity of synthetic Aβ42. The cells were incubated for 24 h with a culture medium containing 25 nM Aβ 42 (Cambridge Biosciences), freshly prepared in PBS, with or without 10% CnLs (20 μg/ml final concentration). The cell viability was assessed by the MTT test. Each assay included a control and two treated conditions (Aβ alone or with CnLs), the experiments being carried six times in triplicates. In order to take into account the inter-assay variability, the cellular viability was expressed as a percentage of the paired control. Comparison between the two treated conditions relied on a *t*-test on the viability values expressed in percentage of controls (degree of freedom = 5 for the 6 assays).

Aβ secretion in cell culture

The concentration of Aβ peptides 40 and 42 was determined by means of a human ELISA kit (Invitrogen) on the supernatant of $hAPP_{sw}$ SH-SY5Y cells, after 24 h of culture in a medium depleted of fetal calf serum (FCS) in order to eliminate the exogeneous Aβ.

Alzheimer disease cases

AD patients were enrolled in a brain donation program of the Brain Bank "GIE NeuroCEB" run by a consortium of Patients Associations (including France Alzheimer Association). The patient himself, or the next of kin, had signed the consent form, in accordance with the French Bioethical Laws. The project had been approved by the scientific committee of the Brain Bank. Samples from the superior temporal gyrus (Brodmann area 22), around 4 cm^3 in volume, were mounted on a cork piece with Cryomount embedding medium and dipped in isopentane cooled by liquid nitrogen. The samples were kept in a deep freezer at −80 °C.

Diagnosis

The diagnosis had been made by experienced neuropathologists using the NIA-AA criteria[20] on samples immunostained by Aβ, tau and ubiquitin antibodies. Only samples from cases with high levels of AD changes and cognitive deficit were used in this study.

CnLs affinity for Aβ deposits in human AD tissue

Sections from temporal isocortex (superior temporal gyrus) and from hippocampus of three AD subjects (Braak neurofibrillary stage VI, Thal phase 5), containing numerous amyloid deposits, were used for the study. Post-mortem frozen 10-μm-thick sections were thawed at room temperature and fixed for 10 min in 100% acetone, then washed three times for 5 min with PBS. The samples were incubated for 30 min with PBS–Tween 0.05% solution. They were abundantly washed with PBS and incubated with a 200-μl suspension of nanoliposomes (20 μg/ml in PBS), for 2 h. Subsequently, the samples were gently washed in PBS and mounted.

Photochemical properties of CnLs

Leica SP2 confocal laser scanning microscope was used for the examination of the tissue. The characteristics of the fluorescence of the CnLs labeling the senile plaques were studied by testing different excitation wavelengths (405, 488, 543 and 633 nm) and by collecting the emitted signal at short successive intervals of wavelengths. The most efficient excitation wavelength was 488 nm and was systematically used for the detection of CnLs labeling in further experiments. Sections of tissue stained with FITC nanoliposomes were also examined with a 488-nm excitation wavelength.

CnLs labeling of all Aβ deposits

A double-labeling experiment using CnLs and Aβ immunohistochemistry was performed to determine which types of Aβ deposits were labeled. After acetone fixation and PBS washing, the sections were incubated for 4 h in 200-μl solution of 6F3D anti-Aβ antibody (Dako), at 1/200 dilution. The samples were washed three times with PBS and incubated for 2 h with the secondary antibody bearing the chromogen red Cy3. Following the immunostaining, the samples were further washed in PBS before incubation with CnLs, for 2 h. Colocalization was indicated by a yellow color on the "merged" images.

CnLs labeling of amyloid Aβ deposits

Only some Aβ deposits (such as the core of the senile plaque) are amyloid i.e. Congo red positive, as enriched in β-pleated sheets. In order to determine if the affinity of CnLs was related to that secondary structure, a double-labeling experiment was performed with Congo red. The tissue was first incubated with an alkaline solution of saturated NaCl for 10 min and then in a Congo red solution (3 mg/ml in 80% EtOH saturated in NaCl) for other 15 min. The sample was further washed abundantly with PBS and incubated for 2 h with CnLs.

CnLs affinity for Aβ deposits on APPxPS1 mouse tissue

The affinity of CnLs for Aβ deposits was investigated in post-mortem tissue of transgenic mice overexpressing AD-related human mutations (APPxPS1 mice) and developing numerous Aβ deposits. Mice were sacrificed with an overdose of sodium pentobarbital and perfused transcardially with a fixative solution containing 4% paraformaldehyde in 125 mM PB (phosphate buffer). After cryoprotection, 40-μm sections were prepared on a freezing microtome and collected in PB. Sections were then incubated for 2 h with 1 ml of CnLs (4 μg/ml).

In vivo affinity of CnLs for Aβ deposits

All in vivo experiments on animals were conducted in accordance with the ethical standards of French and European laws (European Communities Council Directive of 24 November 1986). Both B.D. and I.Y. received official agreements from the French Ministry of Agriculture to carry out research and experiments on animals (including surgery). The affinity of CnLs for Aβ deposits was studied in vivo on the same transgenic mouse model (APPxPS1 line). FITC nanoliposomes were used as fluorescent-negative controls. Ten- and 12-month-old mice were anesthetized with a mixture of 4:3 ketamine/xylazine. CnLs (2 μl of 100 μg/ml suspension) were stereotaxically injected in the right hippocampus and in the neocortex using a nanoinjector coupled to a 10-μl Hamilton syringe. The coordinates of the injection site were adapted from the Franklin and Paxinos atlas.[21] The mice were sacrificed using the same

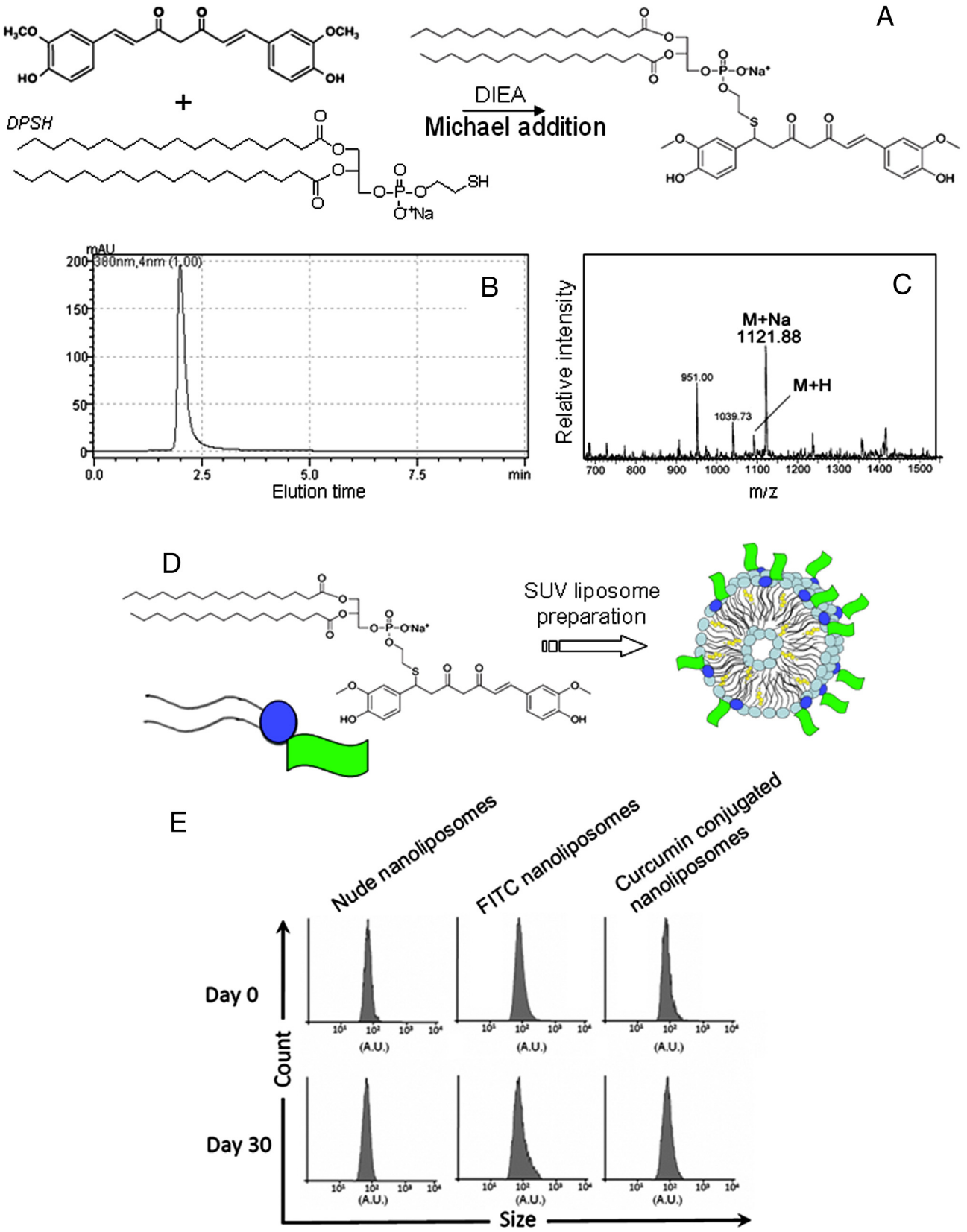

Figure 1. **(A)** DPS–curcumin synthesis via Michael addition; DIEA = *N*,*N*-diisopropylethylamine. **(B)** HPLC analysis of DPS–curcumin. **(C)** Positive ionization mass spectra of the HPLC peak. **(D)** Proposed DPS–curcumin structuring within small unilamelar vesicles (SUV). **(E)** Size stability in time of the nanoliposomes studied by flow cytometry. *x*-axis: A.U. = arbitrary units. The curves were not modified at a time interval of 30 days.

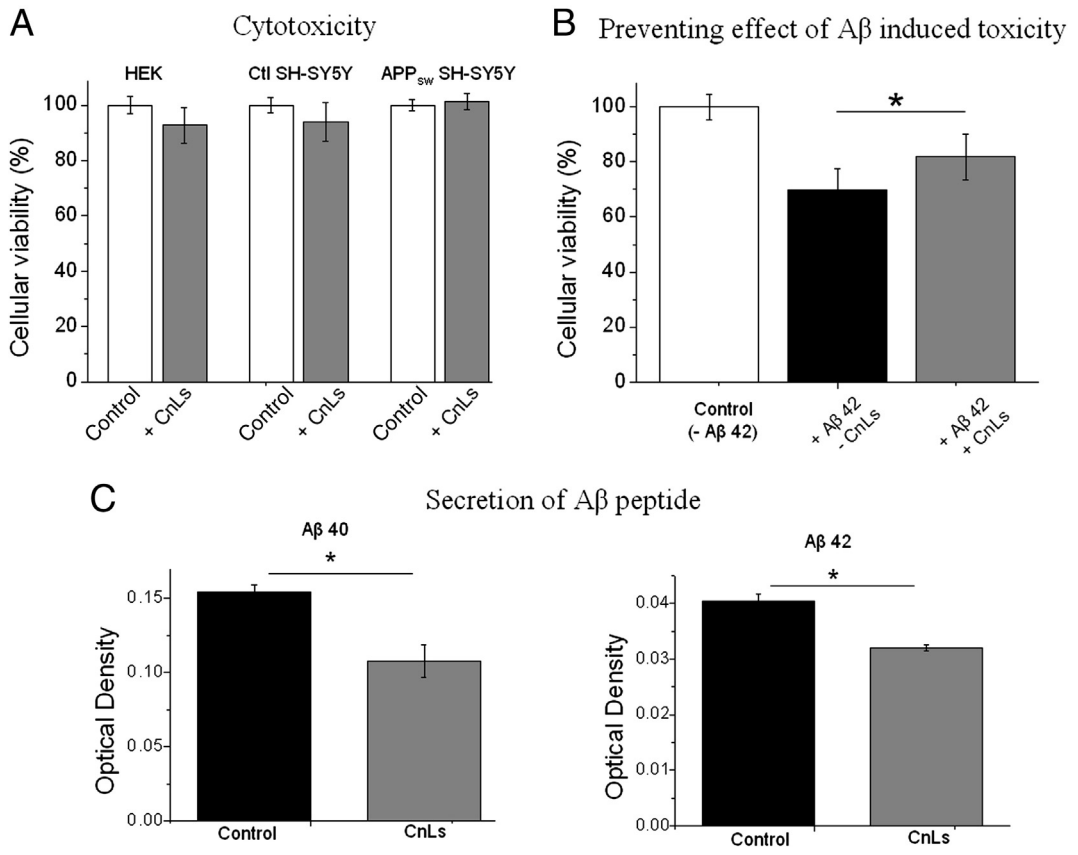

Figure 2. Absence of cytotoxicity of CnLs, prevention of Aβ toxicity and down-regulation of Aβ secretion. **(A)** No significant toxicity ($P>0.6$) on control SH-SY5Y, APP_{sw} SH-SY5Y and HEK cells, after 24 h of incubation with CnLs. **(B)** Significant improvement of cell viability by CnLs after exposure to Aβ 42 ($P<0.028$). **(C)** Significantly reduced concentration of Aβ 40 and 42, ($P<0.05$) in the supernatant of APP_{sw} SH-SY5Y, after 24 h of incubation in a FCS free medium containing CnLs.

protocol as previously, 30 min and 24 h after the injection. The specificity of senile plaques labeled by the CnLs in vivo was confirmed post-mortem by a rapid Congo red staining (to avoid a protracted contact of ethanol with liposomes): 1 min of incubation in an alkaline solution of saturated NaCl and 5 min of incubation in a Congo red solution (3 mg/ml in 80% EtOH saturated in NaCl).

Results

Curcumin–phospholipid conjugate

The synthesis of curcumin–phospholipid conjugate (DPS–curcumin) was performed via Michael addition, as described in Figure 1, *A*. DPS–curcumin was analyzed with NMR, TLC and HPLC followed by ESI-MS. A broad signal corresponding to DPS–curcumin was detected by ^{1}H-NMR (400 MHz, MeOD) δ ppm: 7.47 (d, 1H, J = 15.8 Hz), 7.2-6.7 (m, 6H), 6.55 (d, 1H, J = 15.8 Hz), 5.22-5.12 (m, 1H), 4.6-4.53 (m, 1H), 4.38 (dd, 1H), 4.30-4.11 (m, 3H), 4.04-3.92 (m, 4H), 3.92 (s, 3H), 3,88 (s, 3H), 2.93-2.7 (m, 3H), 2.6-2.49 (m, 1H), 2.3-2.2 (m, 4H), 1.67-1.5 (m, 4H), 1.40-1.20 (m, 48H), 0,90 (t, 6H), OH signal not detected. In $CDCl_3$ a single peak assigned to = C**H**-C(OH)– was also recorded at 5.88 ppm. The peaks detected by ^{13}C-NMR (125 MHz, MeOD) δ ppm confirmed the reaction product (190.6, 182.3, 173.5, 173.2, 147.8, 147.5, 145.5, 145.3, 137.6, 135.0, 128.1, 126.4, 121.7, 120.0, 115.0, 114.6, 111.0, 109.9, 101.5, 70.6, 64.8, 63.4, 62.3, 55.1, 44.8, 33.7, 33.6, 31.7, 31.3, 29.4, 29.3, 29.1, 28.8, 24.6, 22.3, 13.1). TLC analysis showed a single UV/vis, molybdene blue spray and I_2 positive spot ($Rf_{[CHCl3/MeOH\ (4:1)]}$: 0.29). UV absorption was monitored at λmax 380 nm (in $CHCl_3$/MeOH 9:1% with 0.08% TFA). In the same conditions, the non-conjugated curcumin was detected at λmax 420 nm. The HPLC profile showed the presence of only one molecular species (Figure 1, *B*). Positive ESI-MS identified this molecule as a sodium adduct ion of DPS–curcumin (at *m*/*z* 1121.88) (Figure 1, *C*). The curcumin-conjugated nanoliposomes (CnLs) were prepared from 2-dipalmitoyl-*sn*-glycerol-3-phosphatidylcholine (DPPC), cholesterol (Chol) and DPS–curcumin (see Table 1). The proposed structure within the CnLs membrane is presented in Figure 1, *D*.

Physico-chemical properties and size distribution of the nanoliposomes

The mean diameter and ζ-potential of the various nanoliposomes were determined (Table 1). The size of the nanoliposomes increased with the incorporation of curcumin-phospholipids or of FITC, from 63 nm to around 200 nm. The polydispersity index

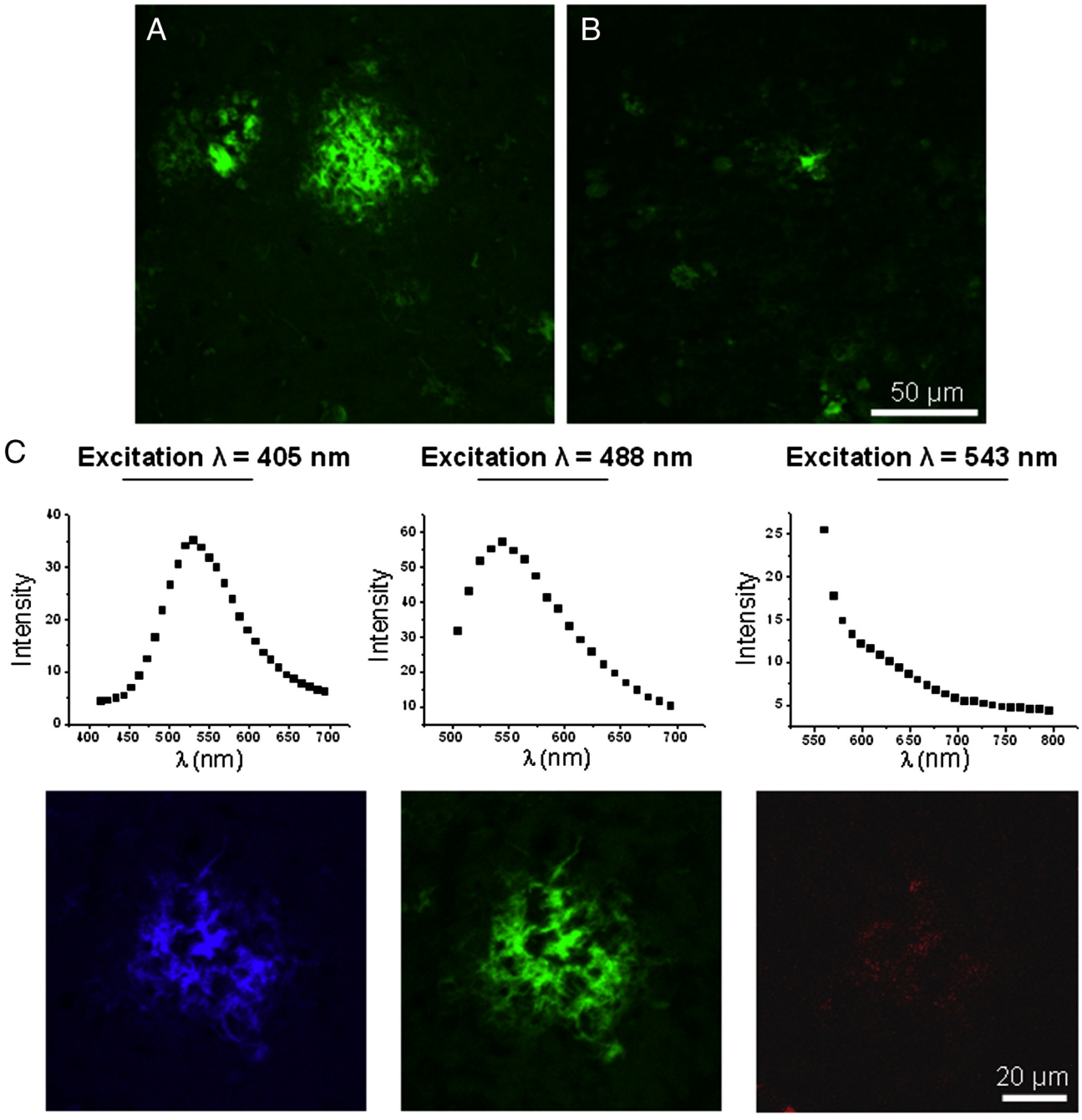

Figure 3. Micrographs of AD brain tissue stained with CnLs. **(A)** Strong staining of amyloid deposits by CnLs. **(B)** Weak, random labeling of the focal deposits by FITC nanoliposomes. **(C)** Fluorescence characteristics of the labeling of the amyloid deposit by CnLs at different excitation wavelengths.

was low (inferior to 0.26) and the surface charge was negative in all cases (ζ-potential from −6.44 to −10.5).

Stability in time of the nanoliposomes

The mean diameter of the nanoliposomes and specifically of CnLs and their ζ-potential, re-assessed after 30 days of storage at 4 °C, were not significantly changed. Flow cytometry confirmed that the particle size distribution of CnLs, FITC nanoliposomes and nude nanoliposomes was monodispersed and stable in time (Figure 1, *E*).

Cellular viability, prevention of Aβ-induced toxicity and down-regulation of Aβ secretion by CnLs

Cytotoxicity of CnLs was evaluated on HEK cell lines, control SH-SY5Y and $hAPP_{sw}$ SH-SY5Y and found to be absent after 24 h of incubation (Figure 2, *A*). The presence of CnLs reduced the cytotoxic effect of Aβ, from 69% of controls to 82%

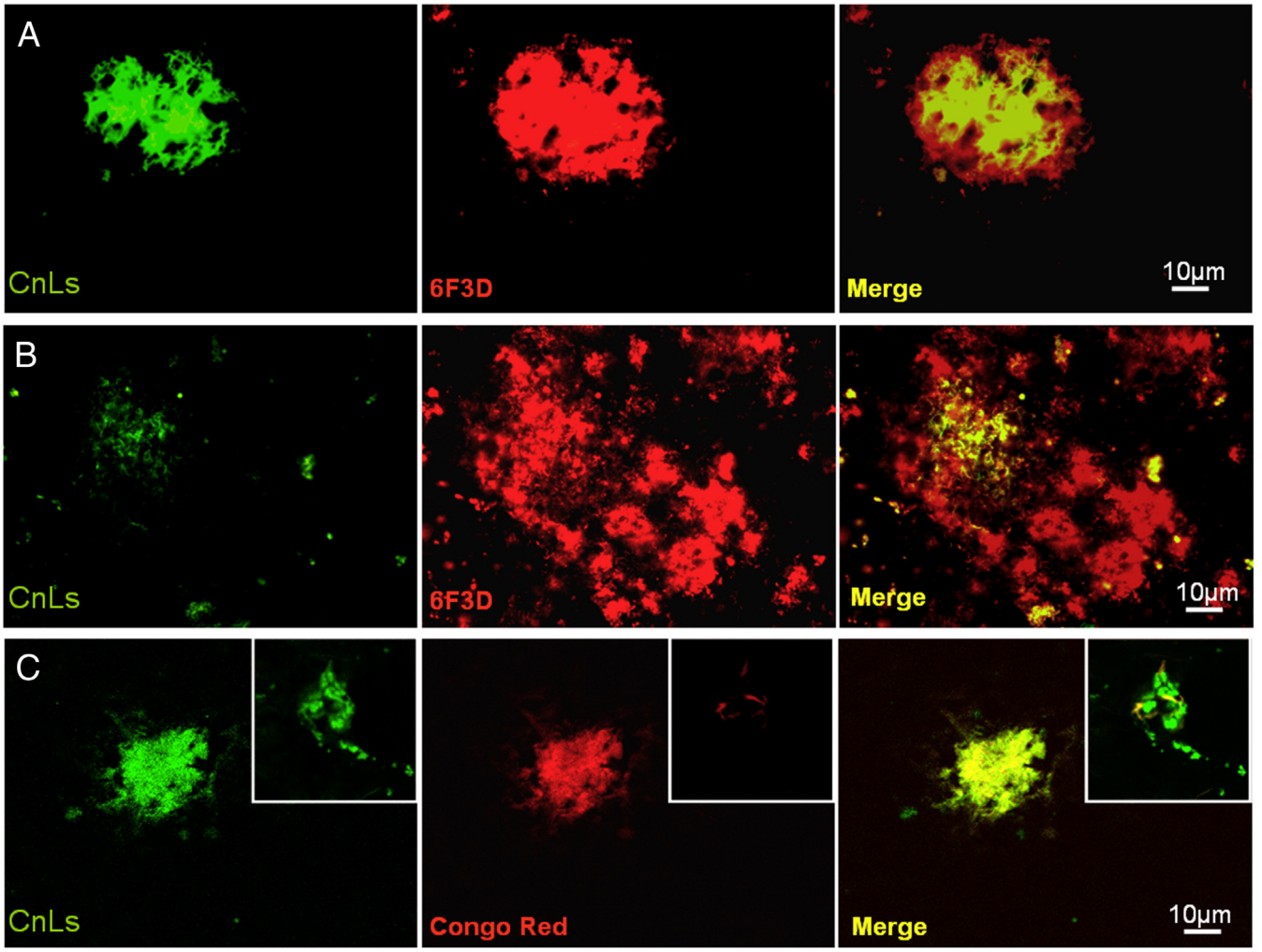

Figure 4. Affinity of CnLs for Aβ deposits (be they amyloid or not). The slides were labeled by curcumin-conjugated nanoliposomes (CnLs), and stained by Congo red (for amyloid Aβ deposits) or immunolabeled by 6F3D anti-Aβ antibody (all Aβ deposits). Core of a senile plaque (**A**), diffuse deposit (**B**) and amyloid Aβ deposit (**C**). Not all the Congo red positive deposits were labeled by CnLs (insert). Colocalization is shown in yellow in the merged image (Merge).

(Figure 2, *B*). The effect was significant, as assessed by a bilateral *t*-test ($t=3.044$, $P<0.029$, $df=5$). Moreover, the concentration of Aβ 40 and 42 evaluated on the supernatant of $hAPP_{sw}$ SH-SY5Y cells, was significantly decreased by 30% ($t=4.3$, $P<0.033$, $df=2$) and 20%, ($t=3.1$, $P<0.015$, $df=2$) respectively, in the presence of CnLs (Figure 2, *C*).

Labeling of the amyloid deposits by the CnLs

CnLs labeled numerous Aβ deposits in human samples (Figure 3, *A*). FITC nanoliposomes (used as a negative control) showed only a weak, random labeling (Figure 3, *B*). Nude nanoliposomes did not give any fluorescent signals.

As it was previously stated that the photochemical properties of curcumin depended on the polarity of its environment,[22–25] the fluorescent properties of CnLs on the brain tissue samples were investigated. The emission signal was collected at different excitation wavelengths: 405, 488, 543 and 633 nm. The signal/noise ratio was low at 405-nm excitation since the autofluorescence of the tissue was significant. The strongest fluorescence emission was recorded at an excitation wavelength of 488 nm: the signal/noise ratio was high, with an emission maximum at 545 nm (Figure 3, *C*). Only residual fluorescence was observed at an excitation wavelength of 543 nm. No signal of senile plaques was collected at 633-nm excitation wavelength. The comparison of the emission spectra of non-conjugated curcumin and CnLs showed a clear shift in the maxima:

$$\text{non}-\text{conjugated curcumin} = 500\ \text{nm vs CnLs} = 530\ \text{nm, at } 405-\text{nm excitation}$$

$$\text{non}-\text{conjugated curcumin} = 520\ \text{nm vs CnLs} = 545\ \text{nm, at } 488-\text{nm excitation.}$$

Lesions stained by CnLs

The percentage of colocalization of CnLs with Aβ immunoreactivity within the senile plaques reached, on average, 70% (Figure 4, *A*). Regarding the amyloid diffuse deposits, only 34% of the Aβ immunoreactivity was also detected by the CnLs (Figure 4, *B*). The Congo red-positive (i.e. amyloid) Aβ deposits

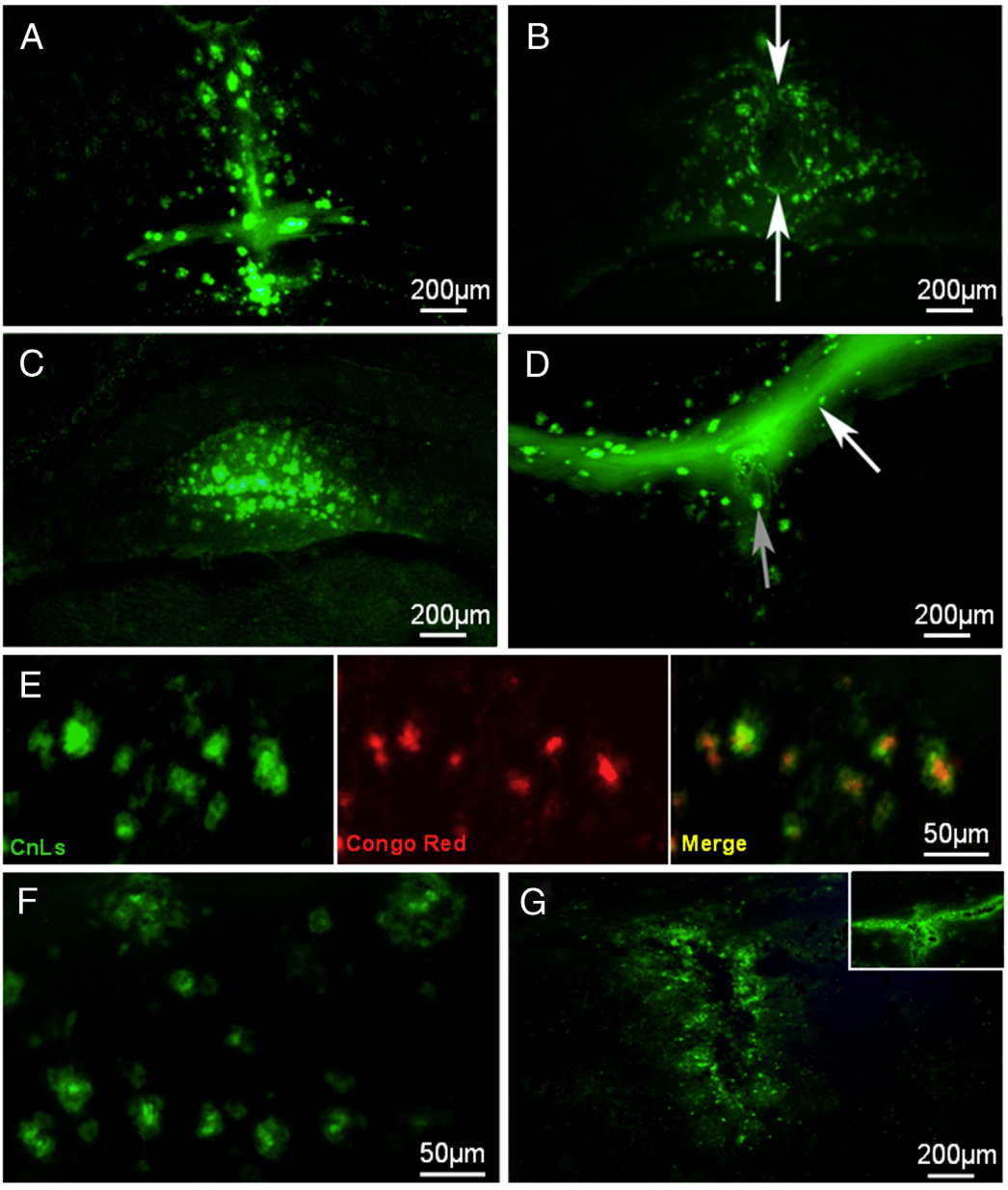

Figure 5. Affinity of CnLs for amyloid deposits in transgenic mice. **(A)** Injection in the neocortex. The injection tract is vertical and surrounded by amyloid deposits labeled by CnLs. Limited lateral diffusion along cortico-cortical fibers is also visible. **(B)** The hole left by the tip of the injection needle is indicated by the arrows. Amyloid deposits are labeled by the CnLs in a sphere of approximately 500 µm in diameter around the tip. **(C)** Labeling of amyloid deposits in hippocampus. **(D)** Diffusion of the labeling along the corpus callosum (white arrow); labeled amyloid deposits are visible next to the corpus callosum (gray arrow). **(E)** Senile plaques which had been labeled in vivo by CnLs (green) were stained post-mortem with Congo red. **(F)** Amyloid deposits stained post-mortem by CnLs in APPxPS1 mice. **(G)** Background fluorescence of the tissue after injection of FITC nanoliposomes; diffusion of nanoliposomes in the corpus callosum (insert).

were also CnLs positive (Figure 4, *C*). Several deposits were singly labeled by CnLs (see Figure 4, *C*, insert).

Affinity of CnLs for Aβ deposits in mice, post-mortem and in vivo

After in vivo stereotactic intracerebral injection of CnLs, Aβ deposits were strongly labeled along the injection tract in the neocortex (Figure 5, *A*). CnLs stained the senile plaques within a spherical region of approximately 500 µm in diameter around the probe tip (Figure 5, *B* and *C*). Some diffusion of the CnLs along the fibers of the corpus callosum was also observed (Figure 5, *D*). The corpus callosum was devoid of fluorescence in brain sections located outside the plane of injection. Congo red, applied on post-mortem sections, stained the plaques previously labeled in vivo by CnLs (Figure 5, *E*). All the Congo red-positive plaques around the injection site were CnLs positive. In vivo and post-mortem labelings of the amyloid deposits by CnLs had similar characteristics (Figure 5, *F*). A

high-fluorescent background was visible around the site of injection of FITC nanoliposomes devoid of curcumin but senile plaques were not labeled (Figure 5, *H*). The FITC-nanoliposomes also diffused along the fibers of the corpus callosum.

Discussion

In this study, CnLs were designed to label amyloid deposits. Curcumin was not encapsulated, but covalently linked to the polar head of phosphatidyl serine. Being available at the external surface of the nanoliposomes, it could directly interact with the amyloid deposits. The mean diameter and ζ-potential values of CnLs were shown to be stable for a period of more than 30 days of storage. CnLs showed no cell toxicity in vitro after 24 h of incubation with different cell lines. They partly prevented Aβ-induced cell death. They were able to down-regulate the secretion of Aβ peptide in cells overexpressing hAPP as already noticed with non-conjugated curcumin.[26] CnLs strongly stained the amyloid deposits in AD post-mortem brain tissue: they labeled approximately 70% of the area and hence of the volume (by Delesse principle)[27] of the senile plaque core and 34% of the volume covered by diffuse deposits. Their high affinity for Aβ deposits was also shown in post-mortem tissue of transgenic mouse model (APPxPS1). Injection in the brain of these mice proved that CnLs could specifically stain Aβ deposits also in vivo. CnLs diffused locally along the injection tract and, on a longer distance, along the fibers of the corpus callosum. This diffusion could be attributed to the nanoliposome carrier, since fluorescent nanoliposomes, devoid of curcumin, showed the same diffusion properties.

Deposition of Aβ is a key feature of familial and sporadic AD. According to the cascade hypothesis,[28] it triggers a series of events that finally induce full-blown AD pathology. In this context, the design of molecules showing high affinity for Aβ could have several uses e.g. histological label, diagnostic markers, possibly therapeutic agents blocking toxicity and favouring clearance. Antibodies of different isotypes and clonality, targeting various epitopes, and diversely modified, have been thoroughly studied. Antibodies have several drawbacks: Aβ being a natural peptide of the self, the antibodies are necessarily autoantibodies with their inherent secondary effects.[29] Moreover, molecular design of monoclonal antibodies is expensive.

Curcumin has attracted attention as a possible alternative. It labels senile plaques in vivo[30,4,31,7] and ex vivo.[30] It was thought to be non-toxic, although this has been recently debated.[32] To overcome the problems raised by the poor hydrosolubility of curcumin and to permit its delivering at specific targets, we, as others,[33–35] developed curcumin nanoliposomes. In the previous attempts,[33–35] curcumin was encapsulated in the liposome. We wanted to use curcumin's affinity for Aβ to target the liposomes to Aβ deposits. This is why curcumin was conjugated to the polar head of one lipid component. Located at the surface of the nanoliposome, it could directly interact with the target. The ability of nanoliposomes to diffuse along fiber tracts (as shown here in the corpus callosum) might be a new mean of carrying diagnostic or therapeutic agents to specific anatomical targets. The mechanism and the usefulness of this transport remain to be explored.

CnLs had a strong affinity for the amyloid deposits on post-mortem AD human and mouse brain tissue, as well as in vivo (as shown here) although, in SPR experiments, the same CnLs did not appear to interact significantly with immobilized synthetic Aβ42 fibrils and monomers.[36] Several factors may explain the discrepancy between the SPR results and our data: it has been previously shown, by thioflavine T assay, that the CnLs interact with synthetic Aβ peptide, inhibiting its aggregation in solution.[37] These data could indicate that the immobilization of the peptide, as in SPR experiments, hinders the interaction. Differences in the structure (conformation) of the naturally formed Aβ aggregates or association of Aβ with other plaque constituents showing a high affinity for curcumin could also be involved.

We are now working on functionalizing the CnLs with molecules that would improve their passage though the BBB and provide a high accessibility to the brain. Our aim will then be to determine to which extent this new formulation will improve the bioavailability of the molecule. It has recently been stressed that the concentration of curcumin reached in the tissue after oral consumption, even at very high dosage, could not match, by several orders of magnitude, in vitro concentration needed to demonstrate beneficial effects.[32,38] CnLs, properly functionalized to cross the BBB could reach the requested concentration in the brain and, adequately loaded with therapeutic or tracing molecules, be useful for the treatment or the diagnosis of AD.

References

1. Hyman BT, Phelps CH, Beach TG, Bigio EH, Cairns NJ, Carrillo MC, et al. National Institute on Aging-Alzheimer's Association guidelines for the neuropathologic assessment of Alzheimer's disease. *Alzheimers Dement* 2012;**8**:1-13.
2. Klunk WE, Engler H, Nordberg A, Wang Y, Blomqvist G, Holt DP, et al. Imaging brain amyloid in Alzheimer's disease with Pittsburgh compound-B. *Ann Neurol* 2004;**55**:306-19.
3. Choi SR, Golding G, Zhuang Z, Zhang W, Lim N, Hefti F, et al. Preclinical properties of 18F-AV-45: a PET agent for Abeta plaques in the brain. *J Nucl Med* 2009;**50**:1887-94.
4. Koronyo-Hamaoui M, Koronyo Y, Ljubimov AV, Miller CA, Ko MK, Black KL, et al. Identification of amyloid plaques in retinas from Alzheimer's patients and noninvasive in vivo optical imaging of retinal plaques in a mouse model. *Neuroimage* 2011;**54**(Suppl 1):S204-17.
5. Lee I, Yang J, Lee JH, Choe YS. Synthesis and evaluation of 1-(4-[(18)F]fluoroethyl)-7-(4′-methyl)curcumin with improved brain permeability for beta-amyloid plaque imaging. *Bioorg Med Chem Lett* 2011;**21**:5765-9.
6. Ray B, Lahiri DK. Neuroinflammation in Alzheimer's disease: different molecular targets and potential therapeutic agents including curcumin. *Curr Opin Pharmacol* 2009;**9**:434-44.
7. Yanagisawa D, Amatsubo T, Morikawa S, Taguchi H, Urushitani M, Shirai N, et al. In vivo detection of amyloid beta deposition using (1)F magnetic resonance imaging with a (1)F-containing curcumin derivative in a mouse model of Alzheimer's disease. *Neuroscience* 2011;**184**:120-7.
8. Costantino L, Tosi G, Ruozi B, Bondioli L, Vandelli MA, Forni F. Chapter 3—colloidal systems for CNS drug delivery. *Prog Brain Res* 2009;**180**:35-69.
9. Jolck RI, Feldborg LN, Andersen S, Moghimi SM, Andresen TL. Engineering liposomes and nanoparticles for biological targeting. *Adv Biochem Eng Biotechnol* 2011;**125**:251-80.

10. Re F, Cambianica I, Sesana S, Salvati E, Cagnotto A, Salmona M, et al. Functionalization with ApoE-derived peptides enhances the interaction with brain capillary endothelial cells of nanoliposomes binding amyloid-beta peptide. *J Biotechnol* 2010;**156**:341-6.
11. Roney C, Kulkarni P, Arora V, Antich P, Bonte F, Wu A, et al. Targeted nanoparticles for drug delivery through the blood–brain barrier for Alzheimer's disease. *J Control Release* 2005;**108**:193-214.
12. Yang H. Nanoparticle-mediated brain-specific drug delivery, imaging, and diagnosis. *Pharm Res* 2010;**27**:1759-71.
13. Webb MS, Rebstein P, Lamson W, Bally MB. Liposomal drug delivery: recent patents and emerging opportunities. *Recent Pat Drug Deliv Formul* 2007;**1**:185-94.
14. Ghaghada KB, Colen RR, Hawley CR, Patel N, Mukundan Jr S. Liposomal contrast agents in brain tumor imaging. *Neuroimaging Clin N Am* 2010;**20**:367-78.
15. Kakinuma K, Tanaka R, Takahashi H, Sekihara Y, Watanabe M, Kuroki M. Drug delivery to the brain using thermosensitive liposome and local hyperthermia. *Int J Hyperthermia* 1996;**12**:157-65.
16. Zhang X, Xie J, Li S, Wang X, Hou X. The study on brain targeting of the amphotericin B liposomes. *J Drug Target* 2003;**11**:117-22.
17. Usta M, Wortelboer HM, Vervoort J, Boersma MG, Rietjens IM, van Bladeren PJ, et al. Human glutathione *S*-transferase-mediated glutathione conjugation of curcumin and efflux of these conjugates in Caco-2 cells. *Chem Res Toxicol* 2007;**20**:1895-902.
18. Stewart JC. Colorimetric determination of phospholipids with ammonium ferrothiocyanate. *Anal Biochem* 1980;**104**:10-4.
19. Mosmann T. Rapid colorimetric assay for cellular growth and survival: application to proliferation and cytotoxicity assays. *J Immunol Methods* 1983;**65**:55-63.
20. Montine TJ, Phelps CH, Beach TG, Bigio EH, Cairns NJ, Dickson DW, et al. National Institute on Aging-Alzheimer's Association guidelines for the neuropathologic assessment of Alzheimer's disease: a practical approach. *Acta Neuropathol* 2012;**123**:1-11.
21. Franklin KBJ, Paxinos G, editors. *The mouse brain in stereotaxic coordinates*. San Diego: Academic Press; 1997.
22. Khopde SM, Priyadarsini KI, Palit DK, Mukherjee T. Effect of solvent on the excited-state photophysical properties of curcumin. *Photochem Photobiol* 2000;**72**:625-31.
23. Kim SH, Gwon SY, Burkinshaw SM, Son YA. The photo- and electrophysical properties of curcumin in aqueous solution. *Spectrochim Acta A Mol Biomol Spectrosc* 2010;**76**:384-7.
24. Mukerjee A, Sorensen TJ, Ranjan AP, Raut S, Gryczynski I, Vishwanatha JK, et al. Spectroscopic properties of curcumin: orientation of transition moments. *J Phys Chem B* 2010;**114**:12679-84.
25. Nardo L, Andreoni A, Bondani M, Masson M, Haukvik T, Tonnesen HH. Studies on curcumin and curcuminoids. XLVI. Photophysical properties of dimethoxycurcumin and *bis*-dehydroxycurcumin. *J Fluoresc* 2012;**22**:597-608.
26. Zhang C, Browne A, Child D, Tanzi RE. Curcumin decreases amyloid-beta peptide levels by attenuating the maturation of amyloid-beta precursor protein. *J Biol Chem* 2010;**285**:28472-80.
27. Weibel. Stereological methods. Practical methods for biological morphometry. London: Academic Press; 1979.
28. Hardy J. Testing times for the "amyloid cascade hypothesis". *Neurobiol Aging* 2002;**23**:1073-4.
29. Orgogozo JM, Gilman S, Dartigues JF, Laurent B, Puel M, Kirby LC, et al. Subacute meningoencephalitis in a subset of patients with AD after Abeta42 immunization. *Neurology* 2003;**61**:46-54.
30. Garcia-Alloza M, Borrelli LA, Rozkalne A, Hyman BT, Bacskai BJ. Curcumin labels amyloid pathology in vivo, disrupts existing plaques, and partially restores distorted neurites in an Alzheimer mouse model. *J Neurochem* 2007;**102**:1095-104.
31. Ran C, Xu X, Raymond SB, Ferrara BJ, Neal K, Bacskai BJ, et al. Design, synthesis, and testing of difluoroboron-derivatized curcumins as near-infrared probes for in vivo detection of amyloid-beta deposits. *J Am Chem Soc* 2009;**131**:15257-61.
32. Burgos-Moron E, Calderon-Montano JM, Salvador J, Robles A, Lopez-Lazaro M. The dark side of curcumin. *Int J Cancer* 2010;**126**:1771-5.
33. Basnet P, Hussain H, Tho I, Skalko-Basnet N. Liposomal delivery system enhances anti-inflammatory properties of curcumin. *J Pharm Sci* 2012;**101**:598-609.
34. Kunwar A, Barik A, Pandey R, Priyadarsini KI. Transport of liposomal and albumin loaded curcumin to living cells: an absorption and fluorescence spectroscopic study. *Biochim Biophys Acta* 2006;**1760**:1513-20.
35. Li L, Braiteh FS, Kurzrock R. Liposome-encapsulated curcumin: in vitro and in vivo effects on proliferation, apoptosis, signaling, and angiogenesis. *Cancer* 2005;**104**:1322-31.
36. Mourtas S, Canovi M, Zona C, Aurilia D, Niarakis A, La Ferla B, et al. Curcumin-decorated nanoliposomes with very high affinity for amyloid-beta1–42 peptide. *Biomaterials* 2011;**32**:1635-45.
37. Taylor M, Moore S, Mourtas S, Niarakis A, Re F, Zona C, et al. Effect of curcumin-associated and lipid ligand-functionalized nanoliposomes on aggregation of the Alzheimer's Abeta peptide. *Nanomedicine* 2011;**7**:541-50.
38. Mancuso C, Siciliano R, Barone E. Curcumin and Alzheimer disease: this marriage is not to be performed. *J Biol Chem* 2011;**286**:le3.